Prograde LWS-KY Transition During Subduction Of The Alpine Continental Crust Of The Sesia-Lanzo Zone: The Ivozio Complex

Michele Zucali

Dipartimento di Scienze della Terra "A. Desio", Università di Milano, Via Mangiagalli 34, I-20133 Milano, Italy
Email: Michele.Zucali@unimi.it

Maria Iole Spalla

Dipartimento di Scienze della Terra "A. Desio", Università di Milano, Via Mangiagalli 34, I-20133 Milano, Italy
CNR-IDPA, Via Mangiagalli 34, I-20133 Milano, Italy

Guido Gosso

Dipartimento di Scienze della Terra "A. Desio", Università di Milano, Via Mangiagalli 34, I-20133 Milano, Italy
CNR-IDPA, Via Mangiagalli 34, I-20133 Milano, Italy

Sonia Racchetti

Regione Lombardia, Via F. Filzi 22, I-201324 Milano, Italy

Fabio Zulbati

Via Camasio 19, I-20157 Milano, Italy

Keywords: lawsonite, kyanite, continental crust, low-T subduction

Abstract: The first occurrence of the lawsonite-kyanite transition is described in the Ivozio complex eclogites of the central Sesia-Lanzo Zone (Western Austroalpine Domain, Italian Alps). The transition from prograde lawsonite to kyanite-bearing eclogites was recorded during a clockwise subduction-exhumation P-T-t-d path. The P-T-t-d evolution of the Ivozio complex is characterized by an Alpine multistage structural and metamorphic re-equilibration: D1 deformation, represented by a penetrative foliation, is the relic of a prograde low-T history, which took place under the epidote-blueschists facies conditions (T = 350 - 500°C and P ≤ 1.2 GPa). Post-D_{1a} re-equilibration stage is marked by the growth of Omp and Lws in eclogites: during this stage T was 520 ± 30 °C at P = 1.4 to 2.2 GPa (eclogite facies conditions). During post-D_{1b} stage the stable association of Omp + Ky + Ep (in lawsonite-eclogites) developed at T 610 ± 20°C and P ≥ 2.0 GPa. This assemblage coincided with Tmax-PTmax conditions. During D2 a penetrative foliation marked by Omp + phengitic/paragonitic white mica + Amp + Ep in eclogites and amphibole-schists was imprinted. In ultramafics (including serpentinites) S2 is widespread as a planar fabric, marked by serpentine + chlorite + amphibole ± ilmenite ± clinopyroxene ± carbonate ± talc . This stage is characterized by temperatures spanning from 500 to 600°C at P ≤ 2.0 GPa. D3 deformation, developed under greenschists facies conditions, is associated with a crenulation cleavage or discrete shear bands.

The early stages of this subduction-exhumation cycle mainly occurred under a low-T regime (i.e. lawsonite-bearing conditions); subsequently the temperature increased (kyanite-eclogite conditions) before the exhumation of the Ivozio complex, marked by the transition to paragonite-eclogite conditions under a steady state thermal regime.

Table of Contents

Introduction

Lawsonite-bearing rocks have been commonly reported from the Alps and from many orogenic belts and subduction complexes as main constituents in the oceanic crust (igneous and sedimentary protoliths) and in trench-related metasediments (e.g. Franciscan: Radvanec et al., 1998; Alps: Bousquet et al., 2004; Reinecke, 1998; Greece: Schliestedt, 1986; Okay, 2002 and Ballevre et al., 2003 and references therein). Lawsonite-bearing rocks are seldomly preserved in the subducted continental crust (Pognante, 1989a; Pognante, 1989b; Pognante et al., 1980; Schwartz et al., 2000), particularly if related to the P-T prograde subduction stages.

Moreover, the reconstruction of the tectono-thermal evolution of slices of continental crust that recorded a low to very low thermal gradient during burial and exhumation, may disclose information about tectonic mechanisms of erosion and dragging to depth of slices of the upper plate continent during active subduction of cold oceanic lithosphere.

In this contribution we investigate the tectono-thermal evolution of lawsonite-bearing metabasics of the Ivozio complex in the Sesia-Lanzo Zone (Austroalpine domain of the Western Italian Alps) and describe the metamorphic reactions leading to the production and breakdown of lawsonite; we deduce from them the sequence of thermal regimes characterising the Alpine subduction-collision stages. The protoliths of the metabasic rocks are pre-alpine gabbros accreted to the Austroalpine continental crust during the Variscan orogenic cycle.

Geological Setting

The Ivozio complex (Pognante et al., 1980) is part of the Eclogitic Micaschists Complex (EMC) of the Sesia-Lanzo Zone (SLZ). The SLZ (Fig. 1) is traditionally separated in two elements (Compagnoni et al., 1977; Dal Piaz et al., 1972): an upper element or "II Zona Diorito-Kinzigitica" (IIDK), comprising metapelites and metabasics with a dominant pre-Alpine metamorphic imprint under amphibolite/granulite facies conditions, and a lower element consisting of polymetamorphic metapelites, metagranitoids and metabasics, with Permian igneous bodies (e.g. Monte Mucrone, Val Sermenza gabbro). The lower element is further divided in three metamorphic complexes: the "Gneiss Minuti Complex" (GMC), showing a dominant Alpine metamorphic imprint under greenschist facies conditions, and the "Eclogitic Micaschists Complex" (EMC), showing a dominant Alpine imprint under eclogite facies conditions and the Rocca Canavese Thrust Sheet (Pognante, 1989a; Pognante, 1989b; Spalla and Zulbati, 2004) lawsonite-blueschists facies metamorphic imprint characterizes the P-retrograde exhumation path.

Figure 1. Location Map

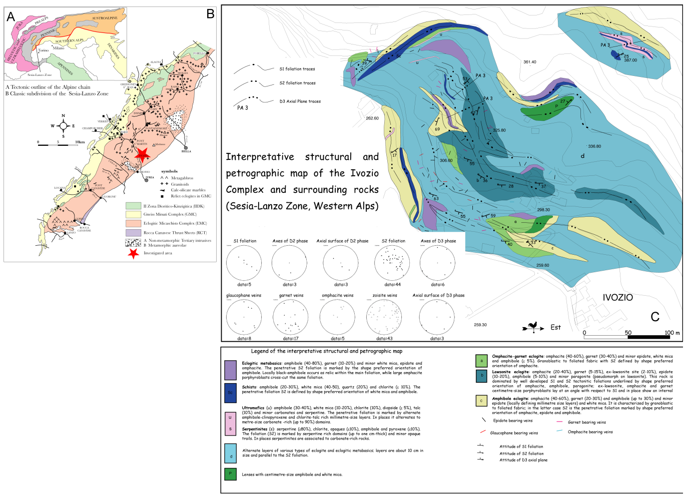

a) Tectonic outline of the Alpine chain with the location of the Sesia-Lanzo Zone;

b) Simplified geological map of the Sesia-Lanzo Zone.

c) Interpretative structural and petrographic map of the Ivozio mafic-ultramafic complex (Austroalpine domain, Sesia-Lanzo Zone, Western Alps): field mapping by S. Racchetti, M.I. Spalla, M. Zucali and F. Zulbati Petrillo. Stereographic projections of main mesoscopic fabric elements.

The structural evolution of the EMC of the SLZ (Table 1) is accomplished during pre-Alpine times under granulite to amphibolite to greenschists facies conditions (Lardeaux, 1981; Lardeaux and Spalla, 1991; Spalla et al., 2005; Zucali, 2002; Zucali et al., 2002) and during Alpine times under prograde blueschists to retrograde greenschists, through eclogite facies peak conditions.

Table 1a. Structural evolution of EMC of the SLZ

References	Pre-Alpine	Blueschists	Eclogite	Blueschists	Greenschists
(1)			D1	D2	D3
(2)		D0	D1	D2	D3
(3)	D0		D1	D2	D3+D4
(4)	D1	D2	D3	D4	D5
(5)	D0		D1 + D2 ----------> D2		
(6)			D1	D2	D3
(7)			D1 + D2 ----------> D2		D3
(8)	D0	D1	D2+D3		D4
(9)	D0		D1+D2	D3	static
(10)	pre-D1	D1 + D2 + D3		D4	D5+D6

Note

Relationships between deformation and metamorphism in the EMC of the Sesia-Lanzo Zone, according to the literature: (1) Gosso, 1977; (2) Pognante et al., 1980; (3) Passchier et al., 1981; (4) Williams and Compagnoni, 1983; (5) Hy, 1984; (6) Ridley, 1989; (7) Ildefonse et al., 1990; (8) Venturini et al., 1991; (9) Inger and Ramsbotham, 1997; (10) Zucali et al., 2002.

The records of pre-Alpine and Alpine evolutions are richer within micaschists and gneisses. During pre-Alpine deformations a penetrative foliation was imprinted within metapelites marked by Crd + Bt + Pl + Kfs + Sill + Grt + Ilm and by Opx + Grt + Pl + Amp + Bt + Ilm in basic granulites (Lardeaux and Spalla, 1991) P - T estimates for the pre-Alpine evolution indicate $0.6 \leq P \leq 0.9$ GPa and T = 700 - 900°C under granulite facies conditions, followed by an amphibolite facies stage (P = 0.3 - 0.5 GPa and T = 570 - 670 °C) and by a greenschist facies re-equilibration (P = 0.25 - 0.35 and T < 550°C) (Lardeaux and Spalla, 1991; Rebay and Spalla, 2001).

The Alpine evolution is characterized by polyphasic deformation under blueschist to eclogite facies conditions followed by retrogression under blueschist to successive greenschist facies conditions (Compagnoni, 1977; Compagnoni et al., 1977; Dal Piaz et al., 1972; Gosso, 1977; Pognante et al., 1980; Tropper et al., 1999; Zucali, 2002; Zucali et al., 2002). The eclogite facies stages occurred at P 2.1 GPa and T 650°C, as inferred by (Tropper and Essene, 2002) on the basis of Ky-occurrence as armoured inclusions in Grt-bearing amphibolites; during blueschists to greenschists facies retrogression km-scale folding of eclogitic foliation occurred, in places associated with a new penetrative foliation. Large scale shear zones developed during final stages of greenschists facies re-equilibration in central SLZ (Handy et al., 2005). Brittle-ductile faulting also occurred during the final stages of the Alpine evolution and assisted intrusion of andesitic dykes and igneous stocks (i.e. Biella-Miagliano and Traversella in Fig. 1).

Absolute age estimates and field relationships (see Table 1b for references and used methods) allowed to attribute an age 270 Ma to the granulite facies stage, an age 240 Ma to the amphibolite facies and an age 170 Ma to the greenschists facies metamorphism. Mineral ages ranging between 60 and 70 Ma have been related to the Alpine eclogite facies peak.

The Ivozio complex (Figure 1) includes eclogitic metabasics, eclogites, lawsonite-eclogites and scarce ultramafics that show layers of metapyroxenites and antigorite serpentinites; a primary igneous layering also exists (Pognante et al., 1980). All lithologies record penetrative Alpine metamorphic imprints, whereas pre-Alpine assemblages are scanty. Pognante et al. (1980) described a pre-eclogitic stage of deformation under blueschists facies conditions with extensive granular scale deformation; B1 and B2 deformation phases developed the main composite foliation and were associated with the wide development of eclogite facies assemblages within all lithologies; Lws growth was doubtfully attributed to B1 structures. B3 large-scale folds occurred under blueschists facies conditions; the Late Alpine evolution ended with a poorly developed stage under greenschists facies conditions. The metabasic protoliths of Ivozio complex have been dated by Rubatto (1998) at 355 ±9 Ma (see Table 1b). The lithologies of the Ivozio complex are mutually folded during eclogite to blueschist facies deformation phases, while a greenschist facies deformation refolds the main contact between the Ivozio complex and the surrounding paraschists and metagranitoids of the EMC (B3 deformation phase in Pognante et al., 1980).

Table 1b. Geochronological data for the SLZ

PRE-ALPINE						ALPINE					
Locality	**Lithology / metamorphic stage**	**Method**	**Mineral**	**Age (Ma)**	**Reference**	**Locality**	**Lithology**	**Method**	**Mineral**	**Age (Ma)**	**Reference**
SLZ Nord	metaporphyrites	U-Pb	Monazite	448 ±5	Romer et al. 1996	Monte Mucrone (EMC)	Eclogite	SHRIMP	Zircon	65 ±5	Rubatto et al. 1999
Ivozio Complex (EMC)	metagabbros	SHRIMP (sensitive high-resolution ion microprobe)	Zircon	355 ±9	Rubatto 1998	Aosta Valley (EMC)	Mi-caschist	SHRIMP	Zircon	65 ±3	"
Cima di Bonze (EMC)	metagabbros	SHRIMP	Zircon	350 ±4	Rubatto 1998	Cima di Bonze (EMC)	Mafic rocks	SHRIMP	Zircon	68 ±7	"
Monte Mucrone	metaintrusive	U-Pb	Zircon	293 +1/-2 286 -28	Bussy et al. 199	Monte Mucrone	Meta-quartz-di	Rb-Sr	White Mica	63 ±1.3	Inger et al. 199

Lithologic Types

Five bulk-rock compositions were distinguished at meso- and microscale: eclogites, eclogitic metabasics, schists, serpentinites and ultramafics. Eclogites (Fig. 2) were also distinguished in Type I eclogites (s.s.); Type II, Lws-bearing eclogites (where Lws is always in lozenge-shape pseudomorphs); Type III, Amp-bearing eclogites. Eclogitic metabasics contain more than 50% of Amp, schists contain mainly Amp- and Chl and ultramafics are composed of Serp and minor Px, opaque minerals and Cc.

Figure 2. Amphibolite and eclogite structure

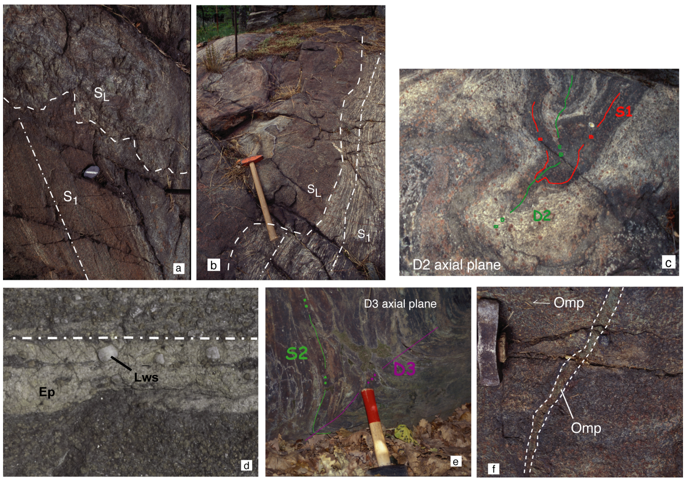

(a and b) S_1 foliation within amphibole-bearing eclogites, marked by SPO of amphiboles, defines an angle (from 0 to 90°) with respect to the SL (original magmatic layering?) between amphibole-bearing eclogites and eclogitic metabasics.

c) S_1 foliation is parallel to SL and defined by dark amphibole-rich eclogite layers and light epidote-rich eclogite layers. D_2 folds bend S_1 foliation.

d) Alternated layers of lawsonite-bearing eclogites and amphibole-bearing eclogites. SL is parallel to S_1 . Lawsonite porphyroblasts, overgrowing S_1 foliation, are characterized by lozenge shape and light colour.

e) D_3 metre scale folding within eclogites.

f) Centimetre thick fracture filled by omphacite; millimetre thick omphacite porphyroblasts occur in a 30 cm-thick zone.

Structural evolution

All lithologies are lenticular in shape and elongate parallel to the dominant S_2 foliation, as shown in Fig. 1.

Six stages of structural evolution have been separated on the base of overprinting relationships: pre-D_1 igneous structures; D_1, D_2 and D_3 ductile deformation phases of Alpine age and fracture systems filled by peculiar mineral assemblages, ascribed to post-D_2 and post-D_3 stages.

Pre-D_1 planar structures (magmatic layering) are tens of centimetres-thick layers of amphibole-bearing eclogites alternate to tens of centimetres -thick layers of Hbl-Grt or Hbl-Grt-Zo/Czo metabasics (Figs. 2a and b). These planar structures are preserved only in metric relict domains.

D_1 consists of a S_1 foliation; it is a mm to cm-spaced foliation, preserved only in metre-size eclogites (Fig. 2) and Amp-schists; S_1 is defined by the Shape Preferred Orientation (SPO) of Amp, Ep and Wm.

D_2 structures are represented by the S_2 foliation, a mm to cm-size differentiated layering. S_2 is marked by SPO of Amp, Ep, ± Omp, ± Wm and ± Chl in eclogites, metabasics and schists; it is a differentiated layering of Srp ± Amp in serpentinites and ultramafics. D_2 rootless folds are centimetre to m-size relics, better preserved in Amp-schists and eclogites (Figs. 1 and 2). S_2 is the most penetrative planar structure at the scale of the Ivozio complex. In eclogites Omp grains, up to cm in size, define a mineral lineation (L_2) within S_2. In syn-D_2 low strain volumes of eclogites, randomly oriented cm-size Omp-Lws and Grt grains overgrow the S_1 foliation marked by a SPO of Amp. An internal foliation, marked by Amp ± Wm, is preserved within Omp and Grt porphyroblasts (Fig. 2). Locally D_3 open folds, refold S_1 and S_2 foliations and lithological boundaries (Figs. 1, 2).

Four types of veins were distinguished on the basis of their mineral composition (Fig. 1 Schmidt diagrams): Omp, Gln, Ep and Grt veins. Overprinting relationships between veins and above described foliations/folds allowed to infer a relative timing:

Grt-bearing veins are generally massive and up to 1 m-length; two orientations exist, generally forming an angle of about 30°. In place Grt-veins display an Omp-rich rim.

Omp-bearing veins are scarce. They cut across the S_1 foliation marked by Amp ± Wm (Fig. 2); close to the Omp fractures (up to 20 cm) Amp underlying the S_1 foliation are replaced by randomly oriented Omp. Omp may be rimmed by aggregates of Gln.

Gln-bearing veins display three principal orientations at about 30° (Fig. 1). They cross cut both S_1 and S_2 foliations. In place Gln may also be rimmed by Omp. These observations lead to the interpretation that at least one generation of Gln veins predate the Omp-bearing veins development.

Ep-bearing veins are characterized by fibrous growth of Ep grains perpendicular to the vein wall. Ep veins may be up to 3 cm in thickness. Locally Ep is intergrown with Gln and may also display rims of Gln and/or Omp.

In places veins filled by Grt, Omp and Gln are reoriented during D_3 folding.

Microstructural evolution

In Fig. 3 the relationships between microstructural evolution and mineral growth have been reported. The record of the multi-stage transformations is more complete in eclogites than in serpentinites, ultramafics and schists.

Figure 3. Deformation scheme

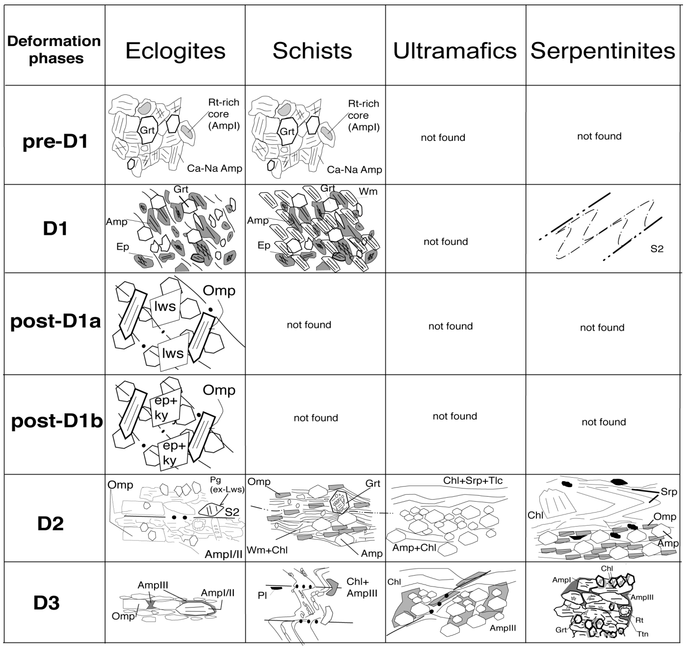

Schematic evolution of fabrics and mineral assemblages in eclogites, schists, ultramafics and sepentinites.

Eclogites

Pre-D_1

Undeformed volumes of TypeIII eclogites preserve the oldest microstructural and mineralogical features, which are brownish Rt-rich cores within Amp and Omp porphyroblasts; Amp Rt-rich cores are rimmed by blue-Amp while the smaller interstitial Omp grains enclose thin aggregates of Rt and oxides in the cores. Brown Amp and interstitial Cpx microstructural site may be interpreted as pre-Alpine remnants according to Compagnoni (Compagnoni, 1977).

D_1 is preserved in TypeIII eclogites as a mineral layering defined by alternate Amp-rich and Ep-rich domains. Amp-rich domains are characterised by SPO of AmpI and WmI defining the S_1 foliation; GrtI porphyroblasts also occur within these layers and the boundaries between AmpI, WmI and GrtI are rational. In places the cores of GrtI porphyroblasts are rich of Qtz + Amp + Rt inclusions. Ep and Wm grains, showing SPO parallel to the mineral layering, constitute Ep-rich domains. Ep grains are elongate and no undulose extinction occurs within these grains. AmpI are large inequant porphyroblasts characterised by slight undulose extinction. In the matrix Rt occurs as isolate grains or aggregates of grains slightly oriented parallel to the S_1 foliation. Qtz is mainly interstitial and is gently oriented parallel to the foliation, showing undulose extinction and deformation lamellae.

The microstuctural relationships allow defining the metamorphic assemblage stable during D_1:

AmpI + GrtI + WmI + Rt + Ep ± Qtz

Post-D_{1a} The coronitic growth of Omp (Figs. 3, 4), Grt and Lws, overprinting the pre-existing S_1 foliation, characterizes this intermediate stage of the mineral growth. Omp are large grains (up to 3 cm) showing an angle with S_1 foliation and displaying inclusions of AmpI, Ep, Rt and Wm, oriented parallel to the external S_1 foliation. Omp grains do not show undulose extinction, deformation twins or lamellae. GrtII porphyroblasts also grew in close relations with Omp. Large (up to 3 cm in size) GrtII poikiloblasts include the S_1 foliation, marked by SPO of AmpI and Ep; Grt rims also include a few randomly oriented Omp grains.

The microstructural features described above allow relating mineral growth to metamorphic reactions in TypeII eclogites:

AmpI + Ep + GrtI = OmpI + GrtII

WmI (Pg) + Ep = Lws + OmpI

leading us to define the new mineral phases growing during post-D_{1a} as:

OmpI + GrtII + Lws

Post-D_1

Lws euhedral porphyroblasts, containing the S_1 foliation marked by SPO of AmpI, Ep and Wm, are completely replaced by pseudomorphs of Ky + Ep (Fig. 3, 4). Ky and Ep do not show any preferred orientation; the inferred breakdown reaction of Lws is therefore:

Lws = Ky + Ep

during this stage the stable metamorphic assemblage is defined by:

Omp + Ky + Ep + Rt ± Qtz

Figure 4. Microstructural relationships within eclogites

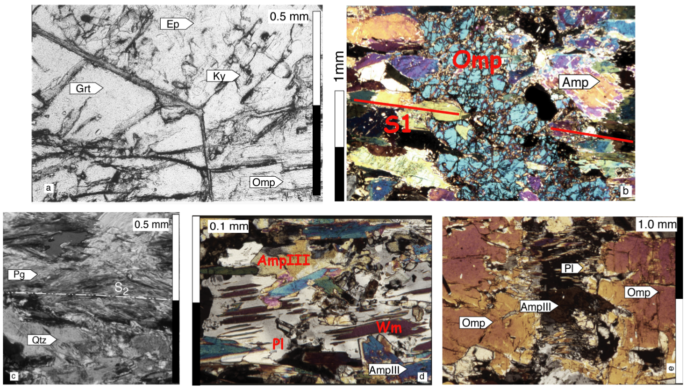

Microphotographs showing microstructural relationships within eclogites.

a) Ep + Ky replacing Lws in contact with Omp and Grt in Lws-eclogites; Ep and Ky do not show any shape preferred orientation. Plane polarised light.

b) Large Omp porphyroblast overgrows at an high angle S_1, underlined by AmpI SPO. Plane polarised light.

c) Pg-Ep aggregate, replacing Lws porphyroblast, is flattened in S_2. Crossed polars.

d) Syn-D_3 aggregates of Pl, Wm and AmpIII rims AmpI/II; boundaries between Pl and AmpIII are rational surface of either phase. Crossed polars.

e) Syn-D_3 micro-fracturing of Omp porphyroblast; an aggregate of AmpIII and Pl fills the micro-fracture neck. Crossed polars.

D_2 is characterised by the development of a penetrative foliation, mainly marked by SPO of Omp, AmpII and Rt or fine-grained Rt aggregates. Omp are elongate grains up to 1 cm in size, showing undulose extinction and deformation bands. S_2 is marked also by AmpII + Ep + Wm; syn-S_2 mineral association is also defined by Grt grains, which show rational boundaries with Omp and AmpII. AmpII show undulose extinction and deformation bands, or occur as small strain-free grains at the rims of the large AmpI porphyroblasts. Ep aggregates mark S_2 , while single Ep grains with undulose extinction may occur either parallel or with an angle with respect to S_2. Aggregates of Wm + Ep, replacing Lws porphyroblasts, are in general re-oriented and flattened parallel to the S_2 foliation (Fig. 3, 4) suggesting that the replacement occurred early in the S_2 development. Wm occurring along the S_2 foliation is characterized by slight undulose extinction.

These microstructures indicate that the assemblage stable during D_2 was:

OmpI + AmpII + Wm + Ep + Rt ± Qtz

and that the disappearing of Ky + Omp assemblages may be explained by the reaction:

Omp + Ky = Amp + Pg + Ep

During D_3 microfolds develop. S_1 and S_2 foliations are gently bent and aggregates of Chl, blue-green AmpIII, Pl and Ep occur (Fig. 4d). In places SPO of AmpIII, Ep and Chl-rich aggregates underline a S_3 axial plane foliation. S_3 also defines discrete shear bands within eclogites, mainly marked by AmpIII and Ep. AmpIII develops as corona of Omp, AmpI and AmpII or grows within Omp syn-D_3 microboudin and microfracture necks associated with Pl (Fig. 4e). Pl also occur as large grains within Pg aggregates. Ttn develops as corona of Rt grains or underlines the S_3 foliation.

These microstructural relationships may be used to suggest the stable assemblage during D_3:

AmpIII + Chl + Pl + Ep + Ttn

due to the interactions of several metamorphic transformations such as

Omp + Qtz + H_2O = Ab + AmpIII

Omp + H_2O = AmpIII + Ep

Cpx + Rt + Wm = Ab + Chl + Ttn +Qtz

Pg = Ab + Qtz + H_2O

Eclogitic metabasics

D_1 is characterized by the S_1 foliation marked by SPO of Amp + Ep + Rt. Grt occur both as porphyroblasts (Fig. 5) and aggregates of small grains. Grt-rich layers are parallel to S_1 . AmpI are large inequant grains, showing undulose extinction and deformation bands. Large AmpI individuals are partially rimmed by an aggregate of smaller strain-free grains (AmpII). AmpII also show SPO parallel to S_1 . Ep grains show slight undulose extinction and their SPO defines S_1 : where Ep occurs at an angle with respect to S_1 , it shows undulose extinction and deformation bands. Rt occurs as isolated grains with SPO slightly parallel to S_1 . Grt is associated to AmpI and Ep within S_1 foliation.

Figure 5. Microstructural relationships within ultramafites

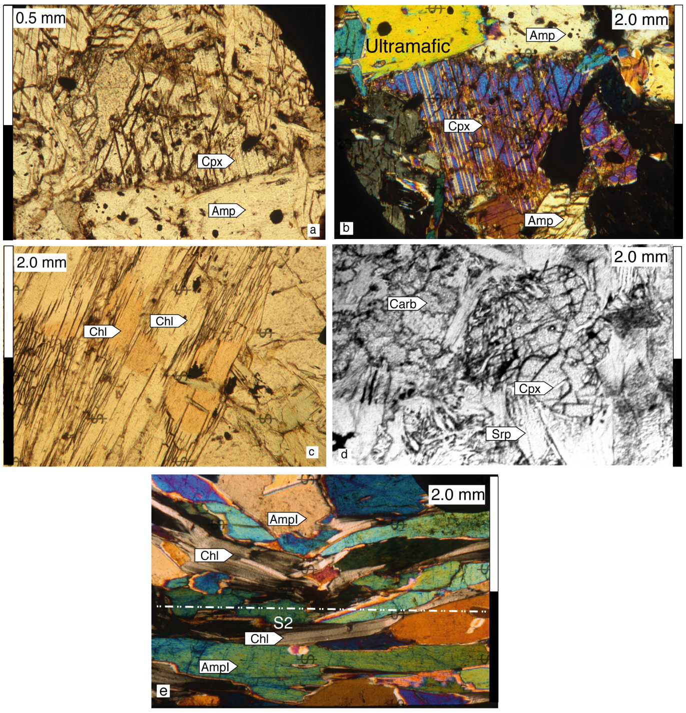

Microphotographs showing microstructural relationships within ultramafites (a-b), serpentinites (c-d), eclogitic metabasics (e).

a, b) Di porphyroblasts rimmed by Amp aggregates. Plane polarised light (a) and crossed polars (b).

c) SPO of Chl aggregates, within serpentinites, defining the S_2 foliation. Plane polarised light.

d) Cpx porphyroblast wrapped by Srp+Chl+Carb aggregates. Plane polarised light.

e) S_2 foliation marked by AmpI and Chl SPO in Eclogitic metabasics. Crossed polars.

The microstructural relationships allow defining the stable assemblage during D_1:

Amp + Grt + Ep + Rt ± Wm ± Qtz

During post-D_1 stage the coronitic growth of large inequant Omp grains occurs. Omp porphyroblasts contain an internal foliation marked by SPO of AmpI and Rt aggregates parallel to S_1 . Grt is also included within Omp porphyroblasts (up to 1 cm in size). Omp lies at a high angle with respect to the S_1 foliation and it is only slightly affected by undulose extinction.

The S_2 foliation is rare within hornblende-rich metabasics; it is defined by AmpII SPO associated with Ep and

Omp. Here Omp shows an intense undulose extinction, deformation bands and, in places, sub-grains. AmpII mainly consist of aggregates of small grains, occurring at the AmpI rims or defining the newly formed foliation. Wm may also occur as single grains showing SPO parallel to S_2 and AmpII.

These microstructural relationships allow defining the stable assemblages during post-D_1 and D_2 :

Amp + Grt + Ep + Omp + Rt ± Wm ± Qtz

During D_3 coronitic transformation widely occur: Chl partially replaces Grt; microboudinaged Omp and Amp are partially substituted by aggregates of Pl + green Amp; Ttn rims Rt. Where S_1 and S_2 are bent Ep occurs within micro-hinges. Micro-shear planes, marked by SPO of Pl + Wm + Chl + Ep crosscut the pre-existing S_1 and S_2 foliations.

The assemblage inferred to be stable during D_3 is:

Green Amp + Pl + Ttn + Wm + Chl + Ep ± Qtz

Amp and Chl-schists

Pre-D_1: The oldest features preserved are brownish Rt-rich cores within Amp porphyroblasts. These relict cores are preserved only in small less deformed volumes of schists.

D_1 is recorded as large inequant AmpI porphyroblasts showing undulose extinction, deformation bands and a shape fabric at an angle (up to 20 degrees) with respect to the dominant S_2 foliation.

The penetrative S_2 foliation is marked by SPO of AmpII + Mg-Chl + Ep + Rt ± Omp . AmpII are strain-free grains characterized by blue-violet pleochroism. Aggregates of Mg-Chl define the S_2 foliation. The boundaries among Amp, Chl and Carbonates are straight. Omp grains are wrapped by AmpII aggregates within Amp-rich domains; Omp shows undulose extinction and deformation bands. Aggregates of carbonates also occur within the S_2 foliation.

The inferred stable assemblage during D_2 is:

Amp + Mg-Chl + Ep + Rt ± Carb ± Wm ± Omp

D_3 is characterised by a gentle folding of S_2; Fe-Chl, Pl and Ttn occur within microfold-hinges.

Ultramafics and serpentinites

Ultramafics are mainly constituted by fine-grained Amp and Cpx, associated with Chl, Rt, carbonates and scarce Tlc and Srp. Brownish cores of Chl and Amp characterise the relict microstructures in ultramafics. Ultramafics do not record D_1 microstructures.

The S_2 penetrative foliation is defined by alternate layers of Chl + Tlc + Srp and Amp + Cpx. Amp and Chl show SPO parallel to the S_2 foliation. Chl has a Fe-Mg-rich core while rims are colourless or with pale-green pleochroism. Cpx (Di) also occur within Amp-rich domains. Amp includes Chl grains without any preferred orientation. Carbonates are interstitial with respect to Amp and Chl. Grain boundaries between Amp, Chl and carbonates are rational.

Serpentinites display a penetrative foliation (S_2) marked by alternate Amp + Cpx + Chl + Carb (layerI) and Srp + Carb + Chl + opaque layers (layerII). Amp and Cpx within layerI show undulose extinction and subgrains but no SPO parallel to the S_2 foliation. Chl within layerI shows a penetrative SPO parallel to S_2 and undulose extinction. Within layerII S_2 is defined by SPO of Chl, Carb and opaque trails; in layerII Srp and Cpx show SPO mainly parallel to S_2 .

The stable assemblage in ultramafics during D_2 is:

Amp + Cpx + Chl + Tlc + Srp

while in serpentinites it is defined by:

Srp + Chl + Carb + opaque ± Amp ± Cpx

Mineral Chemistry

Minerals were analysed with an ARL-SEMQ electron microprobe and natural silicates were used as standards; matrix corrections were calculated with ZAF procedure. The accelerating voltage was 15kV, the sample current 20 nA and beam current 300 nA. Representative mineral compositions are shown in Table 2.

Mineral formula calculations and classifications have been made following the general scheme of Deer et al. (1994), the IMA nomenclature schemes after Leake (Leake et al., 1997) for amphiboles and Yavuz (Yavuz, 2001) for pyroxenes. In Fig. 6 and Table 2 compositional diagrams and mineral analyses for selected mineral phases and bulk rock compositions are reported.

Amphiboles

In eclogites, AmpII and AmpIII were analysed (Fig. 6). AmpII is a Na-Ca amphibole while AmpIII are mainly actinolites (Fig. 6 and Table 2); the Natot content in AmpII is 0.702 a.p.f.u., while it varies from 0.153 to 0.341 a.p.f.u. in AmpIII. The AlVI and NaB contents are higher in AmpII than AmpIII, respectively 0.782 and 0.552 a.p.f.u. in AmpII, from 0.262 to 0.439 a.p.f.u. (AlVI) and from 0.134 to 0.244 a.p.f.u. (NaB) in AmpIII.

Table 2a. Amphibole compositions

Sample	eclogite	eclogite	ultramafite	ultramafite	ultramafite	schists	schists	schists	schists
Name	Na-Ca amp (AmpI)	Actinolite (AmpIII)	Tremolite	Tremolite	Tremolite	Edenite	Magnesiohornblende	Magnesiohornblende	Tremolite
SiO2	55.69	57.37	57.88	57.61	57.15	47.70	50.25	53.69	55.27
TiO2	0.10	0.03	0.00	0.00	0.01	0.18	0.21	0.07	0.05
Al2O3	6.87	1.58	0.01	0.04	0.02	7.91	7.33	2.76	1.33
Cr2O3	0.02	0.01	0.17	0.03	0.07	0.11	0.13	0.36	0.03
MnO	0.06	0.21	0.10	0.08	0.11	0.14	0.12	0.11	0.11
Fe2O3	0.00	0.00	0.00	0.00	0.00	0.00	0.00	0.00	0.00
FeO	6.83	9.55	4.51	3.14	4.98	8.71	8.09	5.01	4.97
ZnO	0.00	0.00	0.00	0.00	0.00	0.00	0.00	0.00	0.00
MgO	16.62	16.79	22.81	22.79	21.34	16.28	18.21	21.17	22.22
CaO	9.81	12.39	12.87	12.79	12.92	11.21	11.59	11.82	12.04
Na2O	2.63	0.56	0.29	0.18	0.28	2.32	2.39	1.32	0.84
K2O	0.10	0.02	0.08	0.03	0.05	0.51	0.53	0.18	0.03
Total	98.73	98.51	98.72	96.69	96.93	95.07	98.85	96.49	96.89
TOTAL	98.73	98.51	98.72	96.69	96.93	95.07	98.85	96.49	96.89
Ox	6.00	6.00	6.00	6.00	6.00	6.00	6.00	6.00	6.00
Si	7.67	8.07	7.85	7.94	7.96	6.97	7.01	7.50	7.62
Al (IV)	0.33	0.00	0.00	0.01	0.00	1.03	0.99	0.45	0.22
Ti (IV)	0.00	0.00	0.00	0.00	0.00	0.00	0.00	0.01	0.01
sum	8.00	8.07	7.85	7.95	7.97	8.00	8.00	7.96	7.84

Figure 6. Compositional variations

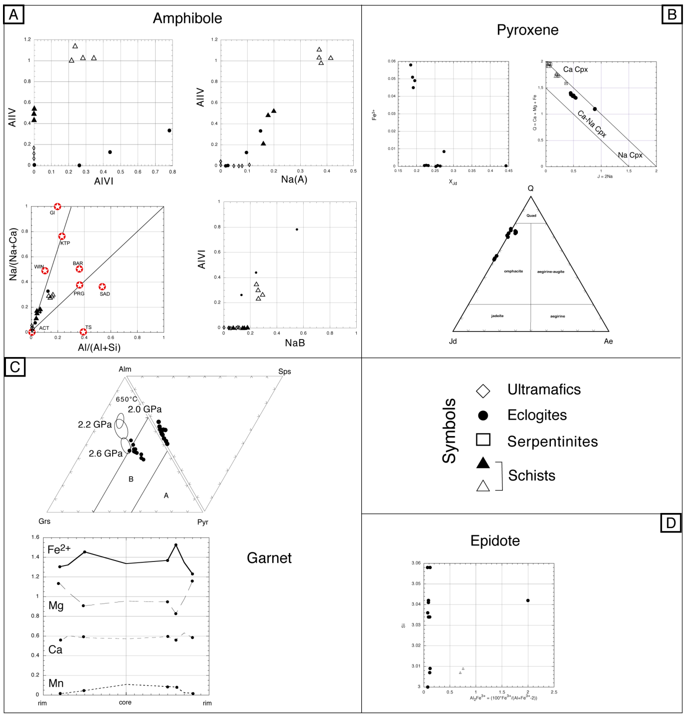

Compositional variations in the amphiboles (A) and clinopyroxene (B) from eclogites, ultramafics, serpentinites and schists. Pyroxene compositions plotted into the Na-pyroxene triangular representation, after Morimoto (1988). C) Compositions of Grt from eclogites. A, B and C are the fields in which plot garnet from different eclogite types according to Coleman (1965). Large ellipses correspond to the composition of Grt synthesised during experiment on basaltic system at 650°C and 2.0-2.2-2.6 GPa from Poli (1993). D) Epidote compositions from eclogites and schists.

In Amp-Chl schists AmpII are mainly magnesio-hornblendes; Natot contents vary from 0.26 to 0.67 a.p.f.u., while CaB varies from 1.70 to 1.78 a.p.f.u.. The differences in Amp composition shown in Fig. 6 most likely correspond to original chemical differences within the wider group of Amp-Chl schists.

In ultramafites Amp are tremolites; Natot content is 0.10 a.p.f.u. CaB content from 1.82 to 1.93 a.p.f.u. and Mg from 4.51 to 4.68 a.p.f.u.

Pyroxenes

OmpI within eclogites show different X^{Jd} content with respect to the microstructural site and to the Fe^{3+} content (Fig. 6) from 0.18 to 0.44 and Fe^{3+} 0.06 a.p.f.u.. The large OmpI porphyroblasts in eclogites show the highest X^{Jd} values, corresponding to lowest Fe^{3+} content; OmpI porphyroblasts within Lws-bearing eclogites show the highest Fe^{3+} contents where OmpI is in contact with Grt and Ep (Fig. 6). OmpI of the Lws-eclogites show the highest Mg contents, ranging from 0.3 to 0.94 a.p.f.u., and the lowest Ca and Na contents (Table 2) with respect to other omphacites in eclogites.

In Amp-Chl schists, Cpx are Ca-rich pyroxenes, with the Na content varying from 0.02 to 0.18 a.p.f.u., Ca from 0.81 to 0.94 a.p.f.u. and Altot from 0.06 to 0.10 a.p.f.u..

In ultramafites and serpentinites Cpx are Di with Ca content from 0.94 to 0.96, Na 0.01 a.p.f.u. and Altot always below 0.01 a.p.f.u..

Table 2b. Pyroxene compositions

Table missing

Garnets

Garnets were analyzed only in eclogites. They show an XCa content varying from 0.19 to 0.23, X_{Mg} (where X_{Mg} =Mg/(Ca+Fe^{2+} Mg+Mn)) from 0.28 to 0.41, X_{Fe} from 0.40 to 0.51 and X_{Mn} 0.04. Grt from Lws-bearing eclogite show compositional variations with an increase of the Fe^{2+} and Ca content from core to rims (Fig. 6).

Table 2c. Garnet and White Mica compositions

Sample	**eclogite**	**lws-eclogite**	**lws-eclogite**	**lws-eclogite**	**lws-eclogite**	**lws-eclogite**	**eclogite**	**lws-wclogite**
Mineral	**grt**	**grt**	**grt**	**grt**	**grt**	**grt**	**white mica**	**white mica**
SiO2	41.17	39.75	38.54	38.63	39.28	40.59	47.96	47.08
Cr2O3	0.01	0.02	0.02	0.03	0.00	0.02	0.00	0.03
Na2O	0.01	0.00	0.00	0.01	0.00	0.00	7.92	7.29
MgO	8.02	10.86	7.10	8.19	9.96	9.20	0.16	0.23
FeO	21.45	19.98	23.40	21.26	20.43	20.77	0.19	0.30
Al2O3	22.04	22.94	21.60	21.79	22.23	22.24	41.61	42.48
K2O	0.01	0.00	0.00	0.00	0.00	0.00	0.32	0.73
CaO	8.61	6.93	6.74	7.14	6.65	7.41	0.44	0.52
TiO2	0.04	0.04	0.06	0.04	0.04	0.03	0.01	0.18
MnO	0.62	0.25	1.24	1.31	0.24	0.33	0.01	0.03
Calc Total	102.01	100.77	98.76	98.42	98.86	100.62	98.63	98.87
Ox-Num	12.00	12.00	12.00	12.00	12.00	12.00	22.00	22.00
Si	3.07	2.96	3.01	3.00	3.00	3.05	5.92	5.81
Al	1.94	2.02	1.99	1.99	2.00	1.97	6.05	6.18
Fe3	0.00	0.06	0.00	0.01	0.00	0.00	0.00	0.00
Fe2	1.34	1.19	1.53	1.37	1.30	1.30	0.02	0.03
Mg	0.89	1.21	0.83	0.95	1.13	1.03	0.03	0.04
Ca	0.69	0.55	0.56	0.59	0.54	0.60	0.06	0.07
Na	0.00	0.00	0.00	0.00	0.00	0.00	1.90	1.74
K	0.00	0.00	0.00	0.00	0.00	0.00	0.05	0.12
Ti	0.00	0.00	0.00	0.00	0.00	0.00	0.00	0.02
Mn	0.04	0.02	0.08	0.09	0.02	0.02	0.00	0.00
Cr	0.00	0.00	0.00	0.00	0.00	0.00	0.00	0.00

Chlorites

Chlorites in ultramafics (Table 2) are characterized by Mg content ranging from 9.14 to 9.72 a.p.f.u., Fetot from 1.07 to 1.61 a.p.f.u., Al from 2.63 to 2.99 a.p.f.u. and Cr from 0.28 to 0.30 a.p.f.u. In serpentinites Mg content varies from 9.78 to 10.09 a.p.f.u., Fetot from 0.79 to 0.81 a.p.f.u., Al from 2.99 to 3.11 a.p.f.u and Cr from 0.08 to 0.10 a.p.f.u. In Amp-Chl schists the Mg content in Chl varies from 6.40 to 8.33 a.p.f.u., Fetot from 1.55 to 3.30 a.p.f.u, Al 3.94 to 4.64 a.p.f.u. and Cr from 0.04 to 0.23 a.p.f.u.

Other minerals

Serpentine shows an Mg content varying from 9.40 to 9.61 a.p.f.u. Fetot from 1.87 to 2.01 a.p.f.u.; the Cr content is always negligible. White micas in eclogites are paragonites: Pg (=Na/(Na+K)) content is higher than 0.93. Fetot and Mg contents are below 0.04 a.p.f.u.. In serpentinites carbonates are characterized by Mg content from 2.69 to 2.88 a.p.f.u. and Fetot from 0.22 to 0.25 a.p.f.u.. In serpentinites the composition are similar to those of serpentinites: Mg content varies from 2.69 to 2.78 a.p.f.u. and Fetot from 0.24 to 0.29 a.p.f.u. Chemical compositions of Wm, Ep, Ky, Oxides, Ttn and Pl are also reported in Table 2.

Table 2d. Epidote compositions

Sample	**lws-eclogite**	**eclogite**	**schists**
Mineral	**epidote**	**epidote**	**epidote**
SiO2	39.67	41.84	37.45
TiO2	0.03	0.05	0.09
Al2O3	33.41	32.94	23.44
Cr2O3	0.02	0.00	1.27
Fe2O3	1.42	2.11	11.21
MnO	0.03	0.00	0.15
MgO	0.06	0.06	0.06
CaO	23.38	24.75	23.06
Na2O	0.00	0.00	0.00
K2O	0.00	0.00	0.00
Totals	98.05	101.78	96.75
Si	3.00	3.06	3.01
Ti	0.00	0.00	0.01
Al	2.98	2.84	2.22
Cr	0.00	0.00	0.08
Fe3	0.08	0.12	0.68
Mn	0.00	0.00	0.01
Mg	0.01	0.01	0.01
Ca	1.90	1.94	1.99
Na	0.00	0.00	0.00
K	0.00	0.00	0.00
Al2Fe	7.64	12.16	75.50

Table 2e. Mineral compositions

Sample	**ul-tram**	**eclo**	**eclo**	**lws-eclogite**	**lws-eclogite**	**serp**	**serp**	**schists**
Mineral	**diopside**	**omphacite**	**omphacite**	**omphacite**	**omphacite**	**diopside**	**diopside**	**diopside**
K2O	0.00			0.26	0.26	0.00	0.00	0.01
CaO	24.34	14.61	14.48	8.50	8.70	24.24	24.75	22.48
TiO2	0.01	0.11	0.11	0.14	0.40	0.05	0.00	0.03
Cr2O3	0.16	0.01	0.00	0.09	0.05	0.00	0.01	0.09
MnO	0.01	0.01	0.02	0.05	0.03	0.32	0.08	0.15
FeOt	2.31	2.86	2.91	4.97	4.86	3.93	1.92	5.48
NiO	0.00	0.00	0.00	0.00	0.00	0.00	0.00	0.00
Na2O	0.17	6.54	6.51	3.51	3.75	0.22	0.13	1.20
SiO2	55.02	58.04	57.04	51.92	52.70	53.43	56.03	53.88
Al2O3	0.00	10.60	10.85	11.66	11.48	0.00	0.01	1.62
MgO	18.00	8.95	8.99	17.50	15.57	16.04	18.28	14.70
TOTAL	100.02	101.73	100.91	98.60	97.80	98.23	101.21	99.64
Si	1.99	2.02	2.00	1.85	1.90	1.99	2.01	1.98
Al.IV	0.00	0.00	0.00	0.15	0.10	0.00	0.00	0.02
Al.VI	0.00	0.44	0.45	0.34	0.39	0.00	0.00	0.05
Ti	0.00	0.00	0.00	0.00	0.01	0.00	0.00	0.00
Cr	0.00	0.00	0.00	0.00	0.00	0.00	0.00	0.00
Fe3+	0.02	0.00	0.00	0.06	0.00	0.03	0.00	0.05
Fe2+	0.05	0.08	0.09	0.09	0.15	0.09	0.06	0.11
Mg	0.97	0.47	0.47	0.93	0.84	0.89	0.98	0.80
Ni	0.00	0.00	0.00	0.00	0.00	0.00	0.00	0.00
Mn	0.00	0.00	0.00	0.00	0.00	0.01	0.00	0.00
Ca	0.95	0.55	0.54	0.32	0.34	0.97	0.95	0.88
Na	0.01	0.44	0.44	0.24	0.26	0.02	0.01	0.09
K	0.00	0.00	0.00	0.01	0.01	0.00	0.00	0.00
Xjd (holland)	-	0.44	0.44	0.18	0.26	-	-	-

Table 2f. Ultramafites

Sample	**Ultramafite**	**Ultramafite**	**Serpentinite**
Mineral	**Opaque**	**Opaque**	**Opaque**
SiO2	0.07	0.07	0.07
Cr2O3	15.25	8.21	5.27
Na2O	0	0	0
MgO	0.07	0.17	0.09
FeO	77.05	82.86	87.56
Al2O3	0	0	0
K2O	0	0	0
CaO	0.12	0.13	0.17
TiO2	0.28	0.15	0.29
MnO	0.37	0.15	0.13
CalcTotal	93.23	91.77	93.6
OxNum	32	32	32
Si	0.02	0.02	0.02
Al	0.00	0.00	0.00
Fe3	12.08	13.85	14.54
Fe2	7.91	7.89	7.95
Mg	0.03	0.08	0.04
Ca	0.04	0.04	0.06
Ti	0.07	0.04	0.07
Mn	0.10	0.04	0.03
Cr	3.74	2.04	1.28

Table 2g. Serpentinites

Sample	Serpentinite	Serpentinite
SiO2	41.34	41.05
Cr2O3	0.05	0.05
Na2O	0.00	0.00
MgO	31.92	32.52
FeO	11.86	11.38
Al2O3	0.66	1.13
K2O	0.00	0.01
CaO	0.04	0.02
TiO2	0.01	0.01
MnO	0.19	0.15
CalcTotal	86.14	86.37
Si	8.17	8.07
Fe2	1.96	1.87
Mg	9.40	9.54
Ca	0.01	0.00
K	0.00	0.00
Ti	0.00	0.00
Mn	0.03	0.03
Cr	0.01	0.01

Thermo-barometric Estimates

Mineral assemblages stable during successive deformations and classical thermo-barometrical estimates have been used in order to define the physical conditions of the evolving metamorphism. Thermo-barometers were only applied to mineral pairs in mutual contact and with rational boundaries.

Pressure and temperature stability fields of metamorphic assemblages or reaction equilibria were calculated using Thermocalc (Holland and Powell, 1990) and Perplex (Connolly, 1990). Activities for Thermocalc calculations were obtained using Ax (Holland and Powell, 2000).

T - estimates have been obtained using the calibrations of the Grt-Cpx thermometer (Ai, 1994; Ellis and Green, 1979; Krogh, 1988; Krogh, 2000; Powell, 1985; Sengupta et al., 1989) widely applied also to eclogite facies rocks (see Carswell and Harley, 1990). Grt-Cpx thermometer, applied to the post-D_{1a} , post-D_{1b} and syn-D_2 pairs of Grt-OmpI, in eclogites and Lws-bearing eclogites, yields a T interval of 550 ± 80°C for P from1.5 to 2.0 GPa; according to Phillippot and Kienast (Philippot and Kienast, 1989) the large interval of temperature, obtained using Grt-Cpx thermometer, may be due to the dependence of the estimated temperature with respect to Fe^{3+} content in OmpI. The thermometer based on the Ti content in amphiboles (Otten, 1984) has been applied to Amp-Chl schists, giving results spanning between 570 ± 10°C. Minimal P can be estimated applying the barometer calibrated on the basis of the X^{Jd} content of omphacites in eclogites (Carswell and Harley, 1990; Holland, 1980). This calibration applied to the Omp underlying the S_2 foliation of eclogites gives a P of 1.5 ± 0.1 GPa.

T and P of the superposed metamorphic assemblages are also constrained by the comparison with existing petrogenetic grids and recalculated grids using internally consistent datasets (Connolly, 1990; Holland and Powell, 1990): the pressures attained during the D_1 stage can be constrained by the omphacite-in reaction reported by Poli (Poli, 1993; Poli and Schmidt, 1995) in basaltic system (Fig. 7).

The univariant reactions AmpI + Ep + GrtI = OmpI + GrtII + Pg + Qtz, Omp + Ep + Grt = Lws + Grt and WmI (Pg) + Ep = Lws + OmpI constrain the post-D_{1a} stage, as well the Lws break-down reactions Lws = Ky + Ep and Pg = Omp + Ky + V (Fig. 7).

The post-D_{1b} metamorphic assemblage Omp + Amp + Wm + Ky + Ep + Rt ± Qtz is also constrained by the univariant curves Lws = Ky + Ep and Pg = Omp + Ky + V at P2.0 GPa and T600°C

The D_2 stage is constrained by the univariant reactions Omp + Ky ± V = Pg ± Ep ± Amp, Lws = Ep + Ky and by the general omphacite-in reaction in eclogites: in figure 7 the reactions defining the stability field for D_2 paragenesis, and their references, are reported.

The reactions Ank + Amp + H_2O = Chl + Cpx + CO_2 and Dol + Amp + H_2O = Chl + Cpx + CO_2 (calculated using Thermocalc) for ultramafites also agree with the P-T interval of the syn-D_2 assemblages.

Syn-D_3 retrograde evolution can be well constrained in eclogites by the breakdown of OmpI (aJd=0.4) following the reactions Jd + Qtz = Ab, Omp + Grt = Amp + Grt + Ep and by the Grt-in reaction after Liu et al. (1996).

Figure 7. P-T-d-t path

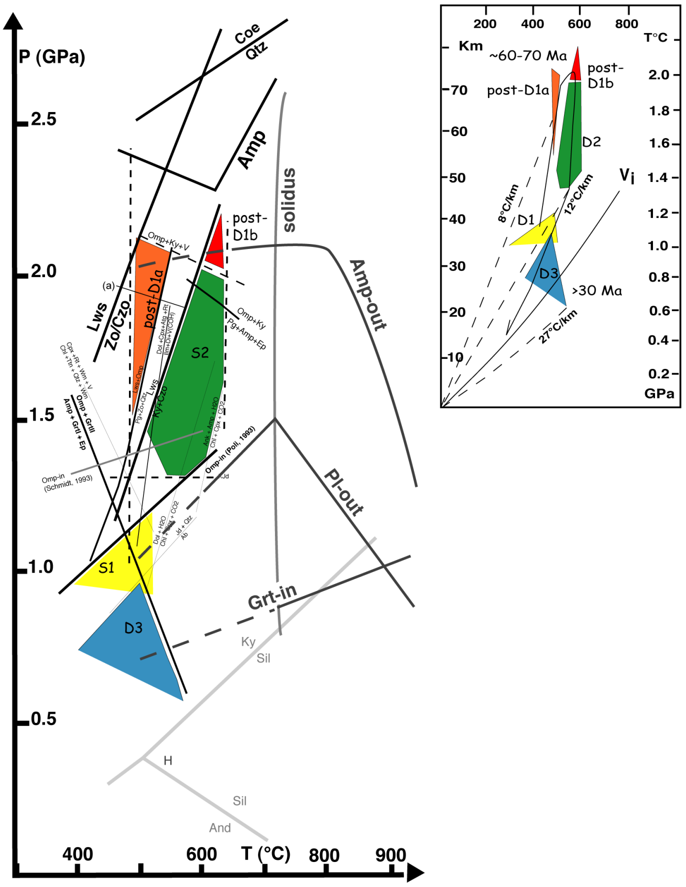

A) P-T-d-t path of the Ivozio complex rocks where coloured boxes represent P-T conditions estimated with respect to successive deformation stages (e.g. D_1, post-D_{1a} and post-D_{1b}). The reactions of amphibole decomposition (Amp-out), of plagioclase disappearance (Pl-out) and of garnet appearance (Grt-in) and the wet solidus are after the experiments of Liu et al. (1996) on the olivine-normative basalt-H_2O system at the amphibolite to eclogite transition; Amp, Zo/Czo and Lws stability fields are after Poli and Schmidt (1995) and Schmidt and Poli (1998). Ky = Sil, And = Sill and And = Ky are after Spear (1993); Omp-in are after Poli (1993) and Schmidt (1993) respectively for experiments on basaltic and tonalitic systems; the reaction (a) Cpx + Ep + Grt = Lws + Grt after Poli and Schmidt (1997), the reaction Pg = Omp + Ky + V and Lws + Omp = Pg + Zo + Qtz are after Poli (1993). Equilibria Amp + GrtI + Ep = Omp + GrtII and Ab = Jd + Qtz for eclogites have been recalculated using Thermocalc (Holland and Powell, 1990); equilibria Chl + Ttn + Qtz + Wm = Cpx + Rt + Wm + V for schists, Dol + Cpx + Atg + Rt = Ilm + Di + V(COH) for serpentinites and Dol + H_2O = Chl + Cpx +CO_2 , Ank + Amp + H_2O = Chl + Cpx +CO_2 for ultramafites have been calculated using Peprlex (Connolly, 1990). Dashed lines correspond to the T and P intervals inferred with thermo-barometers (see text).

B) P-T-t path of the Ivozio complex compared with successive T/depth ratios and a standard stable geotherm (Vi ; Spear, 1993). Absolute age data referred to successive deformation-metamorphic re-equilibration stages are deduced from literature as discussed in the text.

Metamorphic Evolution

The Alpine structural and metamorphic evolution of the Ivozio complex is reported in Fig. 7. The evolution is characterized by a multistage structural and metamorphic re-equilibration during Alpine time:

a) the D_1 deformation phase represents the relic of the prograde history and is characterized by the development of a penetrative foliation within most of the rocks. D_1 developed at T 500°C at depths below 30 km, in the epidote-blueschists facies conditions. P/T and T/Depth ratios are respectively 2.5*10-3GPa°C-1 and 13°Ckm-1 showing that the during burial of Ivozio complex at depth, the thermal regime was compatible with cold oceanic lithosphere subduction.

b) Post-D_{1a} stage is characterized by the static growth of Omp and Lws in eclogites. During this stage temperatures were 520 ± 30°C at depths from 50 to 70 km. The post-D_{1a} evolution completely developed under eclogite facies conditions and P/T was $4*10^{-3}$GPa°C^{-1}, while T/Depth 8°Ckm^{-1}. During this P-prograde stage the thermal regime is lower, if compared with D_1.

c) During the post-D_{1b} stage the eclogite facies metamorphic association of Omp + Ky + Ep (in Lws-eclogites) was stable at P above 2.0 GPa and T = 610 ± 20°C. P/T ratio was $3*10^{-3}$GPa°C^{-1} while T/Depth 8°C km^{-1}. Ex-Lws pseudomorphs consists of Omp + Ky. This re-equilibration stage testifies a slight increase in T/P ratio, attaining at this stage the higher P conditions.

d) During D_2 a penetrative foliation underlined by eclogites facies association (e.g. Omp + Wm + Amp + Ep in eclogites and Amp-schists) developed. During this stage Ky-Ep pseudomorphic replacement of Lws is substituted by Pg + Ep. In ultramafics and serpentinites S_2 is the widespread planar fabric and is underlined by Srp + Chl + Amp ± Ilm ± Cpx ± Carb ± Tlc. This stage is characterized by T = 550 ± 50°C at depths from 48 to 70 km. P/T ratios were between 2 up to 4*10-3GPa/°C and T/Depth ratios 12°C/km, testifying that during decompression the thermal regime is still low.

e) D_3 took place under greenschists facies conditions and corresponds to the local development of a crenulation cleavage or to discrete shear bands; in low strain domains, newly grown corona aggregates are contemporaneous with syn-D_3 mineral growth in foliated rocks. During D_3 temperatures were 580°C at depths 22 km. P/T ratios were 1*10-3GPa/°C and T/Depth 26°C/km. With respect to the P-prograde path, the temperature values, at same pressure, are slightly higher, even if the T/Depth ratio keeps lower than a standard stable geotherm (e.g. Spear, 1993).

Conclusions

In summary the microstructural investigations on the Ivozio mafic-ultramafic rock complex, based on a detailed foliation trajectory map, allow to re-define the deformation-metamorphism relationships as synthesised in Fig. 3. In particular the Lws-growth has been attributed at the D_{1a} stage, which according to the thermobarometric estimates, occurred during final stages of P-prograde path at T 550°C. The Ky ± Omp syn D_{1b} assemblage marks Tmax-PTmax conditions experienced by the Ivozio rocks, reached as a consequence of quasi-isobaric T-increase. P-T estimates indicate that these rocks belonging to the continental Austraolpine basement were buried at a high depth (70km) at T ≤ 630°C. Following this stage a decrease of P and T is recorded, during the exhumation under low-T conditions, by the development of Pg - Ep syn-D_2 assemblage replacing Ky + Omp + Ep. Syn-D_3 greenschists retrogradation marks the transition to a higher T/Depth ratio during the final stage of exhumation. To unravel the uplift-rate of this SLZ portion, at the end of its Alpine evolution, we need to relate the inferred successive P-T re-equilibration stages to the geochronological data, available in the literature (see Fig. 7 and Table 1b for references). All the available radiometric ages, obtained by minerals or mineral assemblages re-equilibrated under eclogite facies conditions, have been interpreted as age of P - T peak conditions. In this light we can attribute the age interval of 60 and 70 Ma to the post-D_{1b} stage. On the other hand the greenschists syn-D_3 retrogradation in the EMC predates the emplacement of Oligocene intrusives (e.g. Lanza, 1979; Scheuring et al., 1973; Zucali, 2002). Therefore the Ivozio complex accomplished its exhumation path during a time interval of 30-40 Ma, indicating minimal uplift rate of 1.8-2.4 mm year-1.

The P-T prograde evolution (D_1 , post-D_{1a} and post-D_{1b}) and the P-retrograde (D_2) stage are characterised by a thermal state compatible with the subduction of cold (i.e. old) oceanic materials (Cloos, 1982; Cloos, 1993; Peacock, 1996), suggesting that the regime might have been already in a steady state during the prograde stages of subduction, or at least not characterized by a higher T/depth ratio. Effective mechanisms able to subduct the continental litosphere during active oceanic subduction are tectonic erosion and ablative subduction (Gerya et al., 2002; Lallemand, 1999; Tao, 1996), both already invoked to justify the very low thermal regime characterising eclogites developed in continental crust units of the Alps (e.g. Polino et al., 1990; Spalla et al., 1996). The syn-D_3 transition to a higher T/depth ratio may represent the thermal signature of the Alpine collision.

Finally it may be noted that P-T paths inferred for Lws-bearing rocks of the SLZ are quite heterogeneous in shape and versus (Pognante, 1989a; Pognante, 1989b; Pognante, 1991; Spalla and Zucali, 2004): this heterogeneity may indicate that the EMC of SLZ is composed by different tectonic metamorphic units or is the result of strong later thermal heterogeneities in the subduction channel.

Acknowledgements

CNR-IDPA is acknowledged for installation and operation of the EPMA and SEM laboratories. C. Malinverno and G. Chiodi provided respectively thin sections and photomicrographs. Fieldwork was carried out by S.R. during her Tesi di Laurea, supervised by M.I.S. and M.Z.

References

Ai, Y., 1994. A revision of the garnet-clinopyroxene Fe2+-Mg exchange geothermometer. Contribution to Mineralogy and Petrology, 115: 467-473.

Ballevre, M., Pitra, P. and Bohn, M., 2003. Lawsonite growth in the epidote blueschists from the Ile de Groix (Armorican Massif, France); a potential geobarometer. Journal of Metamorphic Geology, 21(7): 723-735.

Bousquet, R. et al., 2004. Explanatory notes to the map: metamorphic structure of the Alps transition from Western to Central Alps. Mitteilungen der Osterreichischen Mineralogischen Gesellschaft, 149.

Bussy, F., Venturini, G., Hunziker, J. and Martinotti, G., 1998. U-Pb ages of magmatic rocks of the western Austroalpine Dent-Blanche-Sesia Unit. Schweizerische Mineralogische und Petrographische Mitteilungen, 78: 163-168.

Carswell, D.A. and Harley, S.L., 1990. Mineral barometry and thermometry. In: D.A. Carswell (Editor), Eclogite facies rocks. Blackie, Glasgow and London, pp. 83-110.

Cloos, M., 1982. Flow melanges: Numerical modeling and geologic constraints on their origin in the Franciscan subduction complex, California. Geological Society of America Bulletin, 93: 330-345.

Cloos, M., 1993. Lithosferic buoyancy and collisional orogenesis: subduction of oceanic plateaus, continental margins, island arcs, spreading ridges and seamounts. Geological Society American Bulletin, 105: 715-737.

Coleman, R.G., Beatty, L.B. and Brannock, W.W., 1965. Eclogites and eclogites: their differences and similarities. Geological Society American Bulletin, 76: 485-508.

Compagnoni, R., 1977. The Sesia-Lanzo zone: high-pressure low-temperature metamorphism in the Austroalpine continental margin. Rendiconti della Società Italiana di Mineralogia e Petrologia, 33: 335-374.

Compagnoni, R. et al., 1977. The Sesia-Lanzo Zone: a slice of continental crust, with alpine HP-LT assemblages in the Western Italian Alps. Rendiconti della Società Italiana di Mineralogia e Petrologia, 33: 281-334.

Connolly, J.A.D., 1990. Multivariable phase diagrams; an algorithm based on generalized thermodynamics. American Journal of Science, 290(6): 666-718.

Dal Piaz, G.V., Hunziker, J.C. and Martinotti, G., 1972. La Zona Sesia - Lanzo e l'evoluzione tettonico-metamorfica delle Alpi Nordoccidentali interne. Memorie della Società Geoligica Italiana, 11: 433-460.

Deer, W.A., Howie, R.A. and Zussman, J., 1994. Introduzione ai minerali che costituiscono le rocce. Zanichelli.

Duchene, S. et al., 1997. The Lu-Hf dating of garnets and the ages of the Alpine high-pressure metamorphism. Nature (London), 387(6633): 586-589.

Ellis, D.J. and Green, D.H., 1979. An experimental study on the effect of Ca upon garnet-clinopyroxene Fe-Mg exchange equilibria. Contribution to Mineralogy and Petrology, 71: 13-22.

Gerya, T.V., Stoeckhert, B. and Perchuk, A.L., 2002. Exhumation of high-pressure metamorphic rocks in a subduction channel; a numerical simulation. Tectonics, 21(6): 11-19.

Gosso, G., 1977. Metamorphic evolution and fold history in the eclogite micaschists of the upper Gressoney valley (Sesia-Lanzo zone, Western Alps). Rendiconti della Società Italiana di Mineralogia e Petrologia, 33: 389-407.

Handy, M.R., Babist, J., Wagner, C., Rosemberg, C. and Konrad, M., 2005. Decoupling and its relation to strain partitioning in continental lithosphere: insight from the Periadriatic fault system (European Alps). In: D. Gapais, J.P. Brun and P. Cobbold (Editors), Deformation Mechanisms, Rheology and Tectonics: from Minerals to the Lithosphere. Geological Society, London, Special Pubblications, pp. 249-276.

Holland, T.J.B., 1980. The reaction albite = jadeite + quartz determined experimentally in the range 600°- 1200°C. American Mineralogist, 65: 129-134.

Holland, T.J.B. and Powell, R., 1990. An enlarged and updated internally consistent thermodynamic dataset with uncertains and correlations: the system K2O-Na20-CaO-MgO-MnO-FeO-Fe2O3-Al2O3-TiO2-SiO2-C-H2-O2. Journal of Metamorphic Geology, 8: 89-124.

Holland, T.J.B. and Powell, R., 2000. Ax.

Hy, C., 1984. Métamorphisme polyphasé et évolution tectonique dans la croûte continentale éclogitisée: les séries granitiques et pélitiques du Monte Mucrone (zone Sesia-Lanzo, Alpes italiennes). Paris VI.

Krogh, E.J., 1988. The garnet-clinopyroxene Fe-Mg geothermometer; a reinterpretation of existing experimental data. Contributions to Mineralogy and Petrology, 99(1): 44-48.

Krogh, R.E., 2000. The garnet-clinopyroxene Fe (super 2+) -Mg geothermometer; an updated calibration. In: J.G. Liou and D.A. Carswell (Editors), Garnet peridotites and ultrahigh-pressure minerals. Blackwell. Oxford, United Kingdom. 2000.

Ildefonse, B., Lardeaux, J.M. and Caron, J.M., 1990. The behavior of shape preferred orientations in the metamorphic rocks: amphiboles and jadeites from the Monte Mucrone Area (Sesia-Lanzo Zone, Italian Western Alps). Journal of Structural Geology, 12, 8: 1005-1011.

Inger, S., Ramsbotham, W., Cliff, R.A. and Rex, D.C., 1996. Metamorphic evolution of the Sesia-Lanzo Zone, Western Alps: time constraints from multi-system geochronology. Contribution to Mineralogy and Petrology, 126: 152-168.

Inger, S. and Ramsbotham, W., 1997. Syn-convergent exhumation implied by progressive deformation and metamorphism in the Valle dell'Orco transect, NW Italy Alps. Journal of Geological Society, London, 154: 667-677.

Lallemand, S., 1999. La Subduction Océanique. Gordon and Brunch Science, Amsterdam.

Lanza, R., 1979. Palaeomagnetic data on the andesitic cover of the Sesia-Lanzo Zone; Western Alps. Geologische Rundschau, 68(1): 83-92.

Lardeaux, J.M., 1981. Evolution tectono-metamorphique de la zone nord du Massif de Sesia-Lanzo (Alpes occidentales): un exemple d'éclogitisation de croute continentale. Paris VI, 226 pp.

Lardeaux, J.M. and Spalla, M.I., 1991. From granulites to eclogites in the Sesia zone (Italian Western Alps): a record of the opening and closure of the Piedmont ocean. Journal of Metamorphic Geology, 9: 35-59.

Leake, B.E. et al., 1997. Nomenclature of amphiboles; Report of the Subcommittee on Amphiboles of the International Mineralogical Association, Commission on New Minerals and Mineral Names. American Mineralogist, 82(9-10): 1019-1037.

Liu, J., Bohlen, S.R. and Ernst, W.G., 1996. Stability of hydrous phases in subducting oceanic crust. Earth and Planetary Science Letters, 143: 161-171.

Morimoto, N., 1988. Nomenclature of pyroxenes. Mineralogical MAgazine, 52: 535-550.

Okay, A.I., 2002. Jadeite-chloritoid-glaucophane-lawsonite blueschists in North-west Turkey; unusually high P/ T ratios in continental crust. Journal of Metamorphic Geology, 20(8): 757-768.

Otten, M.T., 1984. The origin of brown hornblende in the Artfjaellet gabbro and dolerites. Contribution to Mineralogy and Petrology, 86: 189-199.

Passchier, C.W., Urai, J.L., Van Loon, J. and Willimas, P.F., 1981. Structural geology of the Central Sesia-Lanzo Zone. Geologie en Mijnbouw, 60: 497-507.

Peacock, S.M., 1996. Thermal and petrological structure of subduction zones, Subduction: Top to Bottom. Geophysical Monograph. American Geophysical Union.

Philippot, P. and Kienast, J.R., 1989. Chemical -microstructural changes in eclogite-facies shear zones (Monviso, Western Alps, north Italy) as indicator of strain history and the mechanism and scale mass transfer. Lithos, 23: 179-200.

Pognante, U., 1989a. Lawsonite, blueschist and eclogite formation in the southern Sesia Zone (Western Alps, Italy). European Journal of Mineralogy, 1: 89-104.

Pognante, U., 1989b. Tectonic implications of lawsonite formation in the Sesia zone (Western Alps). Tectonophysics, 162: 219-227.

Pognante, U., 1991. Petrological constraints on the eclogite- and blueschist-facies metamorphism and P-T-t paths in the Western Alps. Journal of Metamorphic Geology, 9: 5-17.

Pognante, U., Compagnoni, R. and Gosso, G., 1980. Micro-mesostructural relationships in the continental eclogitic rocks of the Sesia-Lanzo zone: a record of a subduction cycle (Italian Western Alps). Rendiconti della Società Italiana di Mineralogia e Petrologia, 36: 169-186.

Poli, S., 1993. The amphibolite-eclogite transformation: an experimental study on basalt. American Journal of Science, 293: 1061-1107.

Poli, S. and Schmidt, M.W., 1995. H2O transport and release in subduction zones: experimental constraints on basaltic and andesitic system. Journal of Geophysical Research, 100 (B11): 22299 - 22314.

Polino, R., Dal Piaz, G.V. and Gosso, G., 1990. Tectonic erosion at the Adria margin and accretionary processes for the Cretaceous orogeny of the Alps. In: F. Roure, P. Heitzmann and R. Polino (Editors), Deep structure of the Alps. Memoires de la Societe Geologique de France, Nouvelle Serie, pp. 345-367.

Powell, R., 1985. Regression diagnostics and robust regression in geothermometer/geobarometer calibration: the garnet-clinopyroxene geothermometer revised. Journal of Metamamorphic Geology, 3: 231-243.

Radvanec, M., Banno, S. and Ernst, W.G., 1998. Chemical microstructure of Franciscan jadeite from Pacheco Pass, California. American Mineralogist, 83(3-4): 273-279.

Rebay, G. and Spalla, M.I., 2001. Emplacement at granulite facies conditions of the Sesia–Lanzo metagabbros: an early record of Permian rifting? Lithos, 58(3-4): 85-104.

Reinecke, T., 1998. Prograde high- to ultrahigh-pressure metamorphism and exhumation of oceanic sediments at Lago di Cignana, Zermatt-Saas Zone, Western Alps. Lithos, 42 (3-4): 147-189.

Ridley, J., 1989. Structural and metamorphic history of a segment of the Sesia-Lanzo Zone, and its bearing on the kinematics of Alpine deformation in the Western Alps. In: M.P. Coward, D. Dietrich and R.G. Park (Editors), Conference on Alpine tectonics. Geological Society Special Publications. Geological Society of London, London, United Kingdom, pp. 189-201.

Romer, R.L., Schärer, U. and Steck, A., 1996. Alpine and pre-Alpine magmatism in the root zone of the Western Alps. Contribution to Mineralogy and Petrology, 123: 138-158.

Rubatto, D., 1998. Dating of pre-Alpine magmatism, Jurassic ophiolites and Alpine subductions in the Western Alps, Swiss Federal Institute of Technology Zurich, Zurich, 174 pp.

Rubatto, D., Gebauer, D. and Compagnoni, R., 1999. Dating of eclogite-facies zircons; the age of Alpine metamorphism in the Sesia-Lanzo Zone (Western Alps). Earth and Planetary Science Letters, 167(3-4): 141-158.

Ruffet, G., Gruau, G., Ballevre, M., Feraud, G. and Philippot, P., 1997. Rb-Sr and (super 40) Ar- (super 39) Ar laser probe dating of high-pressure phengites from the Sesia Zone (Western Alps); underscoring of excess argon and new age constraints on the high-pressure metamorphism. Chemical Geology, 141(1-2): 1-18.

Scheuring, B., Ahrendt, H., Hunziker, J.C. and Zingg, A., 1973. Paleobotanical and geochronological evidence for the Alpine age of the metamorphism in the Sesia-Zone. Geologische Rundschau, 63: 305-326.

Schliestedt, M., 1986 Eclogite-blueschist relationships as evidenced by mineral equilibrium in the high pressure metabasic rocks of Sifnos (Cycladic Islands), Greece. Journal of Petrology, 27: 1439–1459.

Schmidt, M.W., 1993. Phase relations and compositions in tonalite as a function of pressure: an experimental study at 650°C. Am. J. Sc., 293: 1011-1060.

Schmidt, M.W. and Poli, S., 1998. Experimentally based water budgets for dehydrating slabs and consequences for arc magma generation. Earth and Planetary Science Letters, 163 (1-4): 361-379.

Schwartz, S., Lardeaux, J.M. and Tricart, P., 2000. La Zone d'Acceglio (Alpes cottiennes); un nouvel exemple de croute continentale eclogitisee dans les Alpes occidentales. Comptes Rendus de l'Academie des Sciences, Serie II. Sciences de la Terre et des Planetes, 330(12): 859-866.

Sengupta, P., Dasgupta, S., Bhattacharaya, A. and Hariya, Y., 1989. Mixing behaviour in quaternary garnet solid solution and an extended Elli and Green garnet-clinopyroxene geothermometer. Contribution to Mineralogy and Petrology, 103(223-227).

Spalla, M.I. and Zulbati, F., 2004. Structural and petrographic map of the southern Sesia-Lanzo Zone; Monte Soglio-Rocca Canavese, Western Alps, Italy. Memorie di Scienze Geologiche, 55: 119-127; 1 sheet.

Spalla, M.I. and Zucali, M., 2004. Deformation vs. metamorphic re-equilibration heteroheneities in polymetamorphic rocks: a key to infer quality P-T-d-t path. Rivista Italiana di Mineralogia e Petrologia.

Spalla, M.I., Zucali, M., Di Paola, S. and Gosso, G., 2005. A critical assesment of the tectono-thermal memory of rocks and definition of the tectonometamorphic units: evidence from fabric and degree of metamorphic transformations. In: D. Gapais, J.P. Brun and P. Cobbold (Editors), Deformation Mechanisms, Rheology and Tectonics: from Minerals to the Lithosphere. Geological Society, London, Special Pubblications, pp. 227-247.

Spalla, M.I., Lardeaux, J.M., Dal Piaz G.V., Gosso, G. and Messiga, B., 1996. Tectonic significance of Alpine eclogites. Journal of Geodynamics, 21(3): 257-285.

Spear, F., 1993. Metamorphic phase equilibria and pressure-temperature-time paths, 799pp. pp.

Tao, W.C., 1996. Subduction blowout; an ablative subduction mechanism for the formation of horseshoe arcs. In: Anonymous (Editor), AGU 1996 spring meeting. Eos, Transactions, American Geophysical Union. American Geophysical Union, Washington, DC, United States, pp. 269.

Tropper, P. and Essene, E.J., 2002. Thermobarometry in eclogites with multiple stages of mineral growth: an example from the Sesia-Lanzo Zone (Western Alps, Italy). Schweizerische Mineralogische und Petrographische Mitteilungen, 82: 487-514.

Tropper, P., Essene, E.J., Sharp, Z.D. and Hunziker, J.C., 1999. Application of K-feldspar-jadeite-quartz barometry to eclogite facies metagranites and metapelites in the Sesia Lanzo Zone (Western Alps, Italy. Journal of Metamorphic Geology, 17(2): 195-209.

Venturini, G., Martinotti, G. and Hunziker, J.C., 1991. The protoliths of the "Eclogitic Micaschists in the lower Aosta Valley (Sesia-Lanzo zone, Western Alps). Memorie della Società Geoligica Italiana, 43: 347-359.

Williams, P.F. and Compagnoni, R., 1983. Deformation and metamorphism in the Bard area of the Sesia-Lanzo zone, Western Alps, during subductionand uplift. Journal of Metamamorphic Geology, 1: 117-140.

Yavuz, F., 2001. PYROX: A computer program for the IMA pyroxene calssification and calculation scheme. Computers & Geosciences, 27: 97-107.

Zucali, M., 2002. Foliation map of the “Eclogitic Micaschists Complex” (Monte Mucrone – Monte Mars – Mombarone, Sesia-Lanzo Zone, Italy). Memorie Scienze Geologiche, 54: 86-100.

Zucali, M., Spalla, M.I. and Gosso, G., 2002. Strain Partitioning And Fabric Evolution As A Correlation Tool: The Example Of The Eclogitic Micaschists Complex In The Sesia-Lanzo Zone (Monte Mucrone – Monte Mars, Western Alps Italy). Schweizerische Mineralogische und Petrographische Mitteilungen, 82: 429-454.